Biofilm 5 (2023) 100124

Contents lists available at ScienceDirect

Biofilm

journal homepage: www.sciencedirect.com/journal/biofilm

Anti-infective characteristics of a new Carbothane ventricular assist device driveline

Yue Qu [a,b], David McGiffin [c], Lina Duque Sanchez [d,e], Thomas Gengenbach [d], Chris Easton [d], Helmut Thissen [d], Anton Y. Peleg [a,b,*]

[a] Infection Program, Monash Biomedicine Discovery Institute, Department of Microbiology, Monash University, Clayton, Victoria, 3800, Australia
[b] Department of Infectious Diseases, The Alfred Hospital and Central Clinical School, Monash University, Melbourne, Victoria, 3004, Australia
[c] Department of Cardiothoracic Surgery, The Alfred and Monash University, Melbourne, Victoria, 3004, Australia
[d] Commonwealth Scientific and Industrial Research Organization (CSIRO) Manufacturing, Clayton, Victoria, 3168, Australia
[e] Faculty of Pharmacy and Pharmaceutical Sciences, Monash University, Parkville, Victoria, 3052, Australia

ARTICLE INFO

Keywords:
Ventricular assist device driveline
Anti-infective
Carbothane
Biofilms
Surface chemistry

ABSTRACT

Objectives: Driveline infections are a major complication of ventricular assist device (VAD) therapy. A newly introduced Carbothane driveline has preliminarily demonstrated anti-infective potential against driveline infections. This study aimed to comprehensively assess the anti-biofilm capability of the Carbothane driveline and explore its physicochemical characteristics.

Methods: We assessed the Carbothane driveline against biofilm formation of leading microorganisms causing VAD driveline infections, including *Staphylococcus aureus*, *Staphylococcus epidermidis*, *Pseudomonas aeruginosa* and *Candida albicans*, using novel *in vitro* biofilm assays mimicking different infection micro-environments. The importance of physicochemical properties of the Carbothane driveline in microorganism-device interactions were analyzed, particularly focusing on the surface chemistry. The role of micro-gaps in driveline tunnels on biofilm migration was also examined.

Results: All organisms were able to attach to the smooth and velour sections of the Carbothane driveline. Early microbial adherence, at least for *S. aureus* and *S. epidermidis*, did not proceed to the formation of mature biofilms in a drip-flow biofilm reactor mimicking the driveline exit site environment. The presence of a driveline tunnel however, promoted staphylococcal biofilm formation on the Carbothane driveline. Physicochemical analysis of the Carbothane driveline revealed surface characteristics that may have contributed to its anti-biofilm activity, such as the aliphatic nature of its surface. The presence of micro-gaps in the tunnel facilitated biofilm migration of the studied bacterial species.

Conclusion: This study provides experimental evidence to support the anti-biofilm activity of the Carbothane driveline and uncovered specific physicochemical features that may explain its ability to inhibit biofilm formation.

1. Introduction

The application of mechanical circulatory support (MCS) such as contemporary ventricular assist devices (VADs) has been an important advance in the management of patients with end-stage heart disease [1,2]. The need for a driveline from the pump to the controller and power source confers a high risk for a VAD-associated infection [3]. There is a spectrum of VAD-associated infections ranging from VAD-specific infections such as driveline exit site infection, tunnel infection, pump pocket infection to VAD-related bloodstream infection, and it is likely that the driveline is responsible for the initiation and persistence of these infections [3]. The most common VAD-specific infections are driveline exit site and tunnel infections (Fig. S1) [3,4]. Current antimicrobial and/or surgical treatment strategies are suboptimal in curing driveline infections, highlighting the importance of infection prevention. Widely used preventative strategies include prophylactic peri-operative antimicrobials, diligent wound care and hygiene, and at the time of implantation, not allowing the velour section to project externally beyond

Abbreviations: VAD, Ventricular assist device.

* Corresponding author. Department of Infectious Diseases, The Alfred Hospital and Central Clinical School, Monash University, Melbourne, Australia.
E-mail address: anton.peleg@monash.edu (A.Y. Peleg).

https://doi.org/10.1016/j.biofilm.2023.100124
Received 22 November 2022; Received in revised form 10 April 2023; Accepted 15 April 2023
Available online 17 April 2023

the exit site [3]. The velour section of the driveline is designed to stabilize the driveline in the subcutaneous tissue tunnel and to promote tissue in-growth into the driveline. Despite the application of these anti-infective strategies, infections still occur at a substantial rate of 10–20% annually [5,6]. Very recently, we examined infected drivelines explanted from VAD patients undergoing heart transplant and found that biofilms had migrated long distances up the driveline, with micro-gaps within the driveline velour, implying incomplete tissue integration and a likely pathway for biofilms to spread [7].

Biofilm formation has been proposed as the major cause of local driveline infections [8–10]. A range of biofilm-producing microorganisms have been specifically implicated in driveline infections, including opportunistic bacteria such as *Staphylococcus aureus, Pseudomonas aeruginosa, Staphylococcus epidermidis* and the fungal pathogen, *Candida albicans* [11,12]. Once a biofilm is established on the surface of drivelines, the embedded bacteria or fungi become extremely resistant to antimicrobial treatments [7]. Our previous study examined the interactions between microorganisms and the HeartWare VAD (HVAD) Pellethane® driveline (Medtronic, Minneapolis, USA), and found a predilection of different pathogens for different sections of the driveline. Furthermore, the importance of the subcutaneous tunnel in biofilm formation and migration on the driveline was shown [10].

A new Carbothane® driveline replacing the Pellethane® driveline was incorporated into the HVAD system. Carbothane is a family of medical-grade polycarbonate-based polyurethanes. It was claimed that the Carbothane® driveline had increased durability and higher flexibility when compared with the Pellethane driveline, and it was proposed that the higher flexibility may allow for improved healing of the skin exit site and consequentially lead to a reduction in driveline infections [13]. A preliminary clinical evaluation of the anti-infective performance of the Carbothane driveline supported its infection-resistant potential, however patient numbers were small [14]. In this study, we assessed the anti-infective characteristics of the Carbothane driveline using our established driveline-specific infection assays [10], and further characterized the physicochemical features of the biomaterial that may be associated with its antimicrobial properties. Knowledge gained from this study may be applied to other medical devices for improved anti-infective properties, such as for central venous catheters and permanent pacemakers.

2. Materials and methods

2.1. The Carbothane driveline and microorganisms

Carbothane drivelines were provided by Medtronic Australia. The drivelines were prepared as described previously [10] and cut-outs of ~3 × 5 mm^2 were used to study the microorganism-driveline interactions. Four biofilm-forming reference strains, representing the most common microbial species causing VAD-associated infections, were chosen for this study, including *S. epidermidis* RP62A (ATCC 35984), *S. aureus* ATCC 25923, *P. aeruginosa* PAO1, and *C. albicans* SC5314 [3].

2.2. Early microbial adherence assay, drip-flow biofilm reactor assay and tunnel-based biofilm assay

Three *in vitro* infection assays that mimic different phases and infection micro-environments of driveline infections were adopted for this study. These assays assess driveline pathogen-interactions during the progression of a driveline infection from the skin exit site to deep tissue tunnel and have been described in our previously published study [10].

An early adherence assay was carried out to evaluate the initial attachment of microorganisms to the smooth and velour sections of the Carbothane driveline. A sterile and blank drug filter disk (6 mm) was saturated with 25 μL of microbial suspensions prepared in Muller-Hinton broth (MHB, for *S. epidermidis*, *S. aureus* and *P. aeruginosa*) to a density of OD600 = 0.1, or Roswell Park Memorial Institute medium (RPMI-1640, for *C. albicans*) to a density of OD600 = 1.0. Cut-outs of drivelines, including those from the smooth tube section and the velour section were placed on the saturated filter disks, with convex surface directly contacting the drug filter disk. Sufficient contact between microbial suspension and the driveline convex surface was ensured and unnecessary contact between the microbial suspension and the concave surface and the rough edge of driveline cut-out was cautiously avoided. The set-up was then incubated at 37 °C in a humid chamber for 2 h. The convex surface was washed three times with caution by touching drops of phosphate buffered saline (PBS) in a sterile Petri dish.

A modified drip-flow biofilm reactor assay was set up to allow adhered microorganisms to further grow into mature biofilms [10]. The drip-flow biofilm reactor mimics the skin exit site environment by providing very low shear force, continuous supplies of nutrient and oxygen, and open space for dynamic biofilm growth [10,15]. Reactor apparatus and incubation chambers were set up as described in our previous publication [10] (also see Fig. S2). Driveline cut-outs with attached microorganisms, prepared in the early microbial adherence assay were placed on the top of absorbent pads in the biofilm incubation chamber. 10% tryptic soy broth (TSB, BD Biosciences) as growth media, were pumped through the system at a very low speed of 5 mL/h/channel. Biofilms were allowed to grow for 72 h at room temperature. The samples were removed from the chamber and washed three times with PBS.

In parallel, a tunnel-based interstitial biofilm assay was used to examine microbial biofilm formation on drivelines in an environment that mimics the subcutaneous tunnel, as previously described [10]. Driveline smooth tube or velour cut-outs with adhered microorganisms, prepared as described in the early microbial adherence assay, were incubated in an enclosed agar tunnel at 37 °C for 72 h.

Formation of adherent monolayers and biofilms in all three assays was quantitatively and qualitatively assessed by colony-forming unit enumeration and scanning electron microcopy [10]. These assays were carried out in at least three biological replicates [10].

2.3. Biofilm migration

We have previously shown that microbial biofilms can migrate along drivelines [10] and this may be facilitated by micro-gaps in the surrounding tissue [7]. Here, biofilm migration along the surface of the Carbothane driveline was assessed using a tunnel-based assay with and without micro-gaps. Micro-gaps were prepared by cutting the bottom of the agar tunnel longitudinally with sterile surgical blades (No. 24, Swann-Morton, Sheffield, England). Formation and migration of visible biofilms were monitored using an inverted widefield microscope (Leica DMi8 Live Cell) for 72 h, at 24-h intervals. This assay was carried out in six biological repeats.

2.4. Analysis of the physicochemical properties of the carbothane driveline

X-ray photoelectron spectroscopy (XPS) was used to characterize the surface composition of the driveline materials. XPS analysis was performed using either an AXIS Ultra-DLD or an AXIS Nova spectrometer (Kratos Analytical Ltd, U.K.) equipped with a monochromated Al-Kα X-ray source at a power of 180 W (12 mA, 15 kV). An internal electron flood gun was used to compensate for sample charging during irradiation. All elements presented were identified from low-resolution survey spectra (acquired at a pass energy of 160 eV). The atomic concentrations of the detected elements were calculated using integral peak intensities and the sensitivity factors supplied by the manufacturer. Extraction of the possibly contaminating materials silicon and fluorine on the driveline surface in toluene was attempted and resulted in a reduction rather than a complete removal of these elements from the surfaces. Detailed analysis of the carbon high resolution spectra of the velour was carried

out for the driveline smooth section; analysis of the velour proved to be impossible because of differential sample charging, a common problem when electrically non-conductive materials with a highly irregular rough surface topography are analyzed by XPS.

To compensate for the insufficient specificity of XPS, attenuated total reflection-Fourier transform infrared spectroscopy (ATR-FTIR) was employed to further study the polymer chemistry of the smooth section of the Carbothane driveline. ATR-FTIR spectra were recorded with a Nicolet 6700 (Thermo Scientific, Waltham, Massachusetts, USA) instrument coupled to a diamond detector in order to gain more specific information about chemical structures and functionalities present in the samples. The spectra collected were averages of 64 scans recorded with a resolution of 8 cm^{-1}. Background spectra were blanked using air. The data was processed using OMNIC software provided by the manufacturer. Contact angles were measured to characterize surface wettability of the Carbothane driveline. Samples were cut to approximately 8 mm × 6 mm and mounted flat with the help of metal clamps. Static water contact angles were measured across different samples, using an automated contact angle goniometer (KSV Instruments LTD). A droplet of approximately 13 μL of ultrapure MilliQ water was used. Average contact angles were calculated from 9 measurements, with each measurement recording contact angles on both sides of the droplet. The stiffness of the Carbothane driveline was tested by following the protocol from Imamura *et al.* [16], and the flexure extension was kept at 5 mm. Three repeats of two different sections of the smooth tube were measured.

2.5. Immobilization of biofilm extracellular polymer substance (EPS) matrix to the carbothane driveline

Mature biofilms of *S. aureus* ATCC 25923 and *S. epidermidis* RP62A were grown in 6-well plates with TSB and collected after washing three times with PBS [17]. Biofilm EPS matrix was isolated using the method by Taff *et al.* (2012) [18]. Cut-outs of the Carbothane driveline smooth section were incubated with EPS suspensions in Eppendorf tubes for 24 h at 37 °C. Biofilm EPS immobilized on the driveline surfaces were gently washed with distilled water and stained with Alexa Fluor 555 conjugated Wheat Germ Agglutinin (WGA, 10 μg/mL, 1 h in the dark), followed by imaging with a Leica SP5 confocal laser scanning microscope (CLSM). The fluorescent intensity of immobilized EPS was analyzed with Image J software (NIH, USA). This experiment was carried out in five biological repeats. The Pellethane driveline smooth section cut-outs were included for a comparison.

2.6. Evaluation of antibacterial effects of the carbothane material

For contact killing, the Carbothane driveline smooth section cut-outs were exposed to staphylococcal suspensions of ~5×10^8 CFU/mL for 3 h, using the set-up described in the early adherence assay but allowing more bacterial cells to be attached to the driveline surface. Live/dead BacLight bacterial viability kit (L7007, Invitrogen) in combination with CLSM [19] was used to examine the viability of staphylococcal cells upon contact with the surface of the Carbothane driveline. For antibacterial effects mediated by chemicals leached from the Carbothane material, a conventional disk-diffusion susceptibility assay was used to assess the inhibitory effect of the Carbothane driveline against *S. aureus* and *S. epidermidis* [20], replacing the antibiotic disks with Carbothane driveline smooth section cut-outs. Cut-outs of the Pellethane driveline were used for comparative purposes.

2.7. Statistical analysis

To analyze differences in microbial adherence or biofilm formation under different conditions, or EPS immobilization on different drivelines, one-way ANOVA tests or a non-parametric Mann-Whitney test were performed with Minitab Statistical Software 16 for Windows (Minitab Ltd., Coventry, UK) using a significance level of 0.05, depending on the data distribution.

3. Results

3.1. Early adherence of microorganisms to the carbothane driveline

An adherence assay mimicking early-stage microorganism-driveline interactions at the driveline exit site was carried out using four microbial pathogens of VAD driveline infections. After 2-h of incubation, viable counts showed that both the smooth and velour sections of the driveline allowed adherence of all microorganisms, with *P. aeruginosa* attaching to both sections at a significantly greater density than the other species (Fig. 1A). Qualitative SEM supported the viable count results and showed that very few *S. aureus*, *S. epidermidis* and *C. albicans* cells adhered to both sections of the Carbothane driveline in the 2-h incubation period (Fig. 1B).

3.2. The Carbothane driveline resisted staphylococcal biofilm growth

To mimic the skin wound at the driveline exit site and determine whether microorganisms attached to the Carbothane driveline could further develop into mature biofilms in a dynamic environment, a drip-flow biofilm reactor assay was used. After 72-h incubation, viable colony counts were lower for *S. aureus* and *S. epidermidis* (Fig. 2A) compared to that observed at the time of adherence ($P < 0.05$ for both bacteria) (Fig. 1A), and only scant *S. aureus* or *S. epidermidis* cells were seen from either the smooth or velour sections using SEM (Fig. 2B). In contrast, significant numbers of biofilm cells of *P. aeruginosa* and *C. albicans* were isolated from the Carbothane driveline after 72-h incubation in the drip-flow biofilm reactor, especially the velour section with *P. aeruginosa* (Fig. 2A). SEM imaging suggested that *P. aeruginosa* formed monolayer biofilms on the smooth sections and multilayer biofilms on the velour, whereas *C. albicans* grew into small-aggregate biofilms on both sections (Fig. 2B).

3.3. A driveline tunnel promoted biofilm growth on the carbothane driveline

Most VAD driveline infections can readily spread from the skin exit site into the subcutaneous tissue tunnel, along the implanted driveline [7]. A tunnel-based, interstitial biofilm assay was carried out to re-assess microorganism-driveline interactions after invading microorganisms had moved into the subcutaneous tissue tunnel environment. The presence of an agar tunnel significantly promoted biofilm formation of *S. aureus* and *S. epidermidis* on both the smooth and velour sections of the Carbothane driveline, reaching densities of $10^{5.12\text{-}6.75}$ CFU/mm^2 (Fig. 3). *P. aeruginosa* and *C. albicans* also formed substantial biofilms in the tunnel, slightly higher than that formed in the drip-flow biofilm reactor (Figs. 2A and 3).

3.4. The presence of micro-gaps in the tunnel facilitated biofilm migration along the carbothane driveline

We have previously shown that extensive migration of biofilms occurs along infected drivelines in patients with a VAD [7]. Imaging analyses of explanted infected drivelines from patients showed the presence of micro-gaps in the tissue around the driveline in the subcutaneous tunnel [7,10]. We hypothesized that these micro-gaps facilitated more extensive biofilm migration. Here, we assessed whether micro-gaps had any impact on migration of microbial biofilms on the Carbothane driveline using our tunnel-based interstitial biofilm assay. *S. aureus* ATCC 25923, *S. epidermidis* RP62A and *C. albicans* SC5314 all showed limited migration along the Carbothane driveline in a tightly enclosed tunnel, with no migration observed for *P. aeruginosa* PAO1 (Fig. 4A). In contrast, the fabrication of micro-gaps at the driveline-tunnel interface significantly promoted biofilm migration of

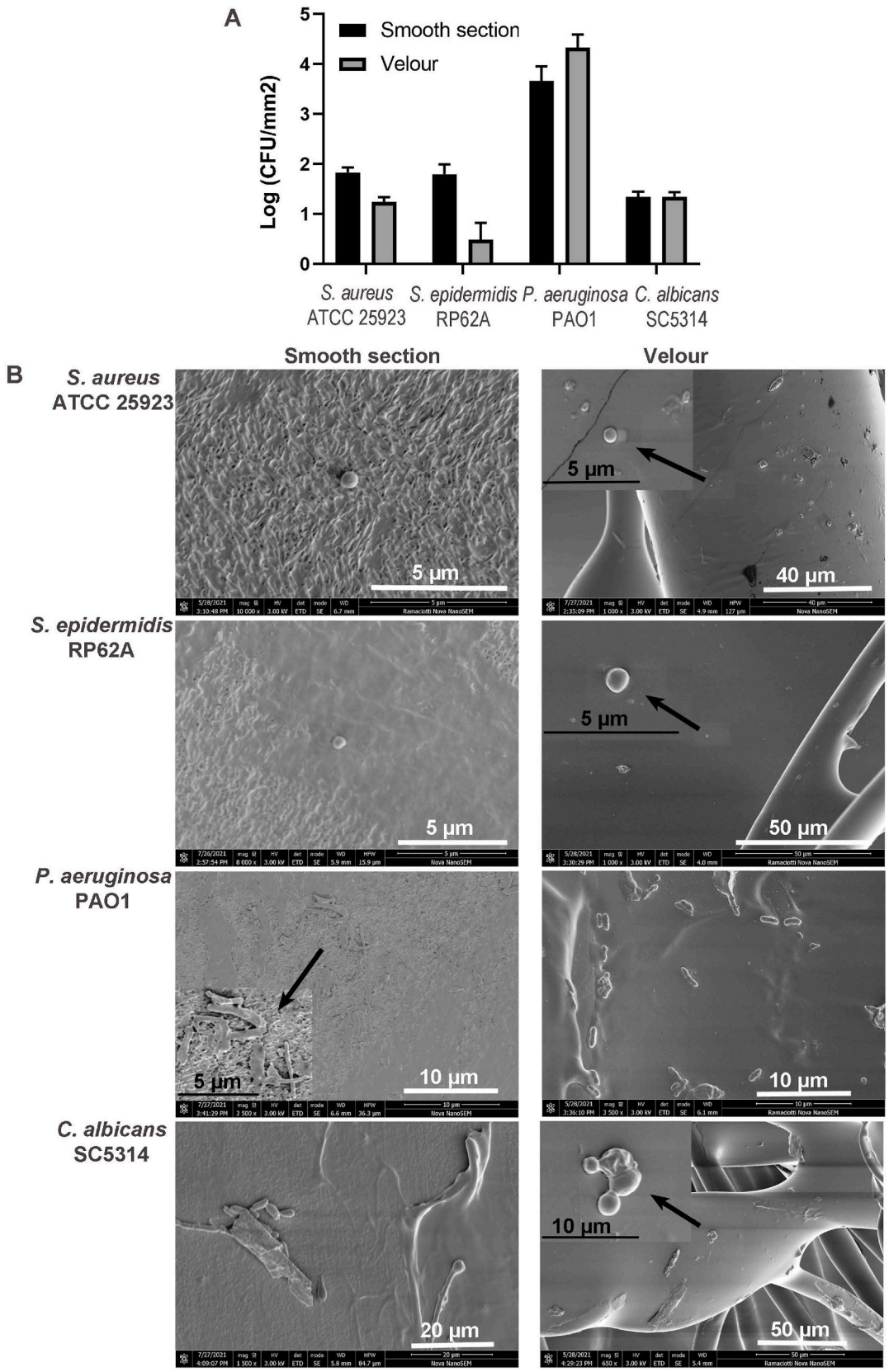

Fig. 1. Early adherence of model microorganisms to different sections of the Carbothane driveline. The adherent growth was allowed for 2 h. A) Quantitative analysis using viable counts, B) Qualitative analysis using scanning electron microscopy (SEM). The experiment was repeated in four biological repeats for viable counts (A) and two biological repeats for SEM (B). Means ± standard errors of the mean (SEM) were presented in Fig. 1A.

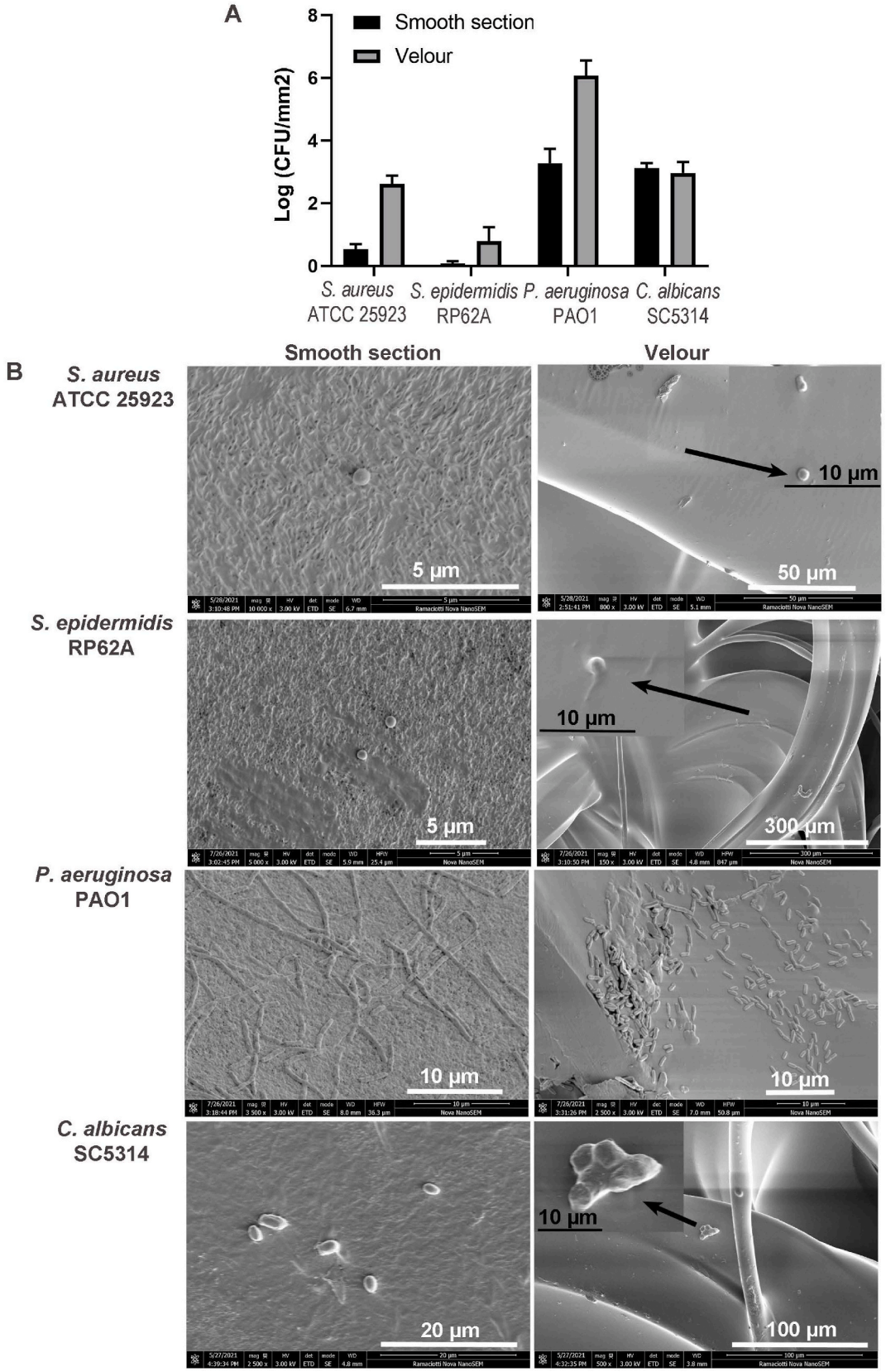

Fig. 2. Biofilm formation of microorganisms on different sections of the Carbothane driveline in a drip-flow biofilm reactor. Biofilm growths were allowed for 72 h. The experiment was biologically repeated four times for viable counts (A) and twice for SEM (B). Means ± standard errors of the mean (SEM) were presented in Fig. 2A.

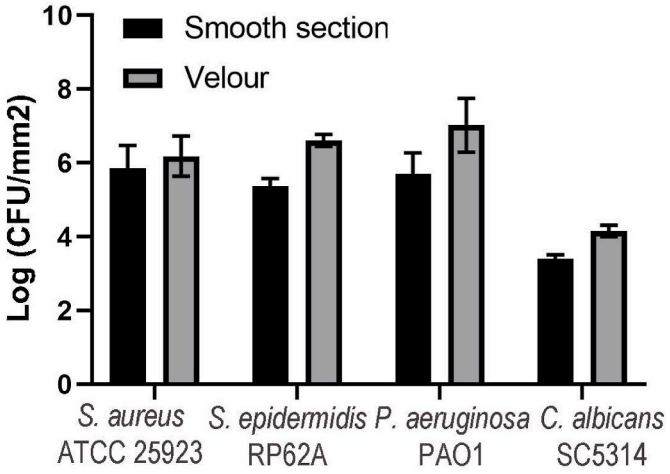

Fig. 3. Biofilm formation of microorganisms on different sections of the Carbothane driveline in a driveline tunnel. The experiment was biologically repeated four times. Means ± standard errors of the mean (SEM) were presented.

S. aureus, *S. epidermidis* and *P. aeruginosa* (Fig. 4B and C), but not for *C. albicans* SC5314 (Fig. 4A and B).

3.5. Physicochemical characteristics of the carbothane driveline

The surface chemistry of biomaterials, including the presence of specific elements and their chemical state can influence their antimicrobial properties [21,22]. To investigate whether the physicochemical features of the Carbothane driveline may explain some of its antimicrobial properties, we used a multi-modal approach of XPS and ATR-FTIR spectroscopy to study the surface composition and polymer chemistry of the driveline. Low energy resolution XPS provides qualitative and quantitative information on the elements present on the biomaterial surface. XPS survey spectra obtained from the smooth and velour sections of the Carbothane driveline indicated the presence of oxygen, nitrogen and carbon as expected for a polyurethane (Table 1). High levels of silicon (Si) and fluorine were also detected (Table 1). High energy resolution XPS gives information on the chemical state and bonding of those elements. The carbon high resolution spectra found a C 1s component with a binding energy of around 290.4 eV that could be assigned to the carbonate group within the Carbothane polymer used for the driveline smooth section (Fig. 5A) [23]. ATR-FTIR spectroscopy confirmed the carbonate nature of the polyurethane constituting the driveline smooth section and provided more detailed information of the carbon chemical state (Fig. 5B). Absorptions at 1739, 1242, 955 and 791 cm^{-1} were attributed to the presence of specific carbonate functional groups. The peaks at 1739 and 1242 cm^{-1} confirmed the nonbonded carbonate carbonyl (C=O) and the carbonate oxygen (C–O–C) groups, respectively [24]. Such infrared spectra suggested aliphatic nature of the polymers used for the driveline smooth section [25]; the ring structure of aliphatic polymers has been associated with biomaterial resistance to bacterial attachment [26]. Other driveline features and surface physicochemical characteristics possibly associated with the low incidence of driveline infections were also examined. We assessed surface wettability of the Carbothane driveline. Both smooth and velour sections were highly hydrophobic, with the smooth section surface having a contact angle of 106.8 ± 4.4 and the velour surface having a contact angle of 126.1 ± 5.3. Outer diameters and bending stiffness are known driveline-related factors that have been associated with the occurrence of driveline infection in VAD patients. The Carbothane driveline had an outer diameter of 4.7 mm. The bending stiffness of the whole driveline unit was ~3.66 ± 0.08 N, with some variation observed between different examination points, suggesting a rigidity similar to that of the silicone-based HeartMate II driveline (~4 N) [16,27].

3.6. The resistance of the carbothane driveline to staphylococcal biofilm EPS and contact killing of staphylococci may explain its anti-infective potential

A productive interaction between EPS secreted by bacterial cells and specific surface functional groups is a key determinant for staphylococcal biofilm formation on biomaterials [21]. The Carbothane driveline appeared not to support adherent staphylococcal cells to further grow into mature biofilms in the drip-flow biofilm reactor. It was known that both staphylococcal strains used in this study were able to produce poly-β(1–6)-N-acetylglucosamine (PNAG)-based EPS under similar growth conditions [10]. We speculated that the Carbothane driveline smooth section had surface chemistry that rejected the interaction with staphylococcal EPS; such an interaction was essential to anchor the EPS on the driveline surface and further immobilize microcolonies and form mature biofilms. We thus challenged the Carbothane driveline and its predecessor Pellethane drivelines with EPS pre-isolated from mature biofilms of *S. aureus* and *S. epidermidis*. Our CLSM assay using PNAG-specific lectin WGA showed that a significantly larger amount of staphylococcal EPS was immobilized to the smooth sections of the Pellethane driveline than that of the Carbothane driveline (Fig. 6A).

In addition to the interaction between driveline materials and biofilm EPS, we also investigated whether the surface of Carbothane drivelines had direct antibacterial effect against staphylococci. CLSM in combination with live/dead BacLight viability staining showed that a substantial population of staphylococcal cells attached to the Carbothane driveline smooth section cut-outs were killed upon 3-h contact (red signals, Fig. 6B). Very few dead cells were observed on the surface of Pellethane driveline smooth sections; non-specific binding between Syto9 (nucleic acid stain for live cells) and the Pellethane driveline however, made comparison with the Carbothane driveline infeasible (Fig. S3). No chemical-leaching-mediated bacterial inhibition was observed for either the Carbothane or the Pellethane driveline (Fig. S4).

4. Discussion

Advances in driveline design and manufacturing, such as reducing driveline size, increasing driveline flexibility, external anchoring to prevent traction injury and the addition of velour to the driveline, have seen a significant decline in VAD-specific infections [3,16]. Changing the driveline outer sheath from a Pellethane-based biomaterial to the Carbothane-based biomaterial was a very recent intervention that has been claimed to reduce the incidence of driveline infections [13,14,27]. A large-scale, multicenter clinical study would be essential but now infeasible for an accurate assessment of the anti-infective performance of the newly introduced Carbothane driveline as the HVAD has been removed from the market. Despite the withdrawal of the HVAD system we felt that a comprehensive *in vitro* investigation of the new Carbothane material was relevant in the context of applications with other medical devices.

The Carbothane driveline was assessed for its capability to support early microbial adherence and biofilm formation using *in vitro* assays that mimic different infection micro-environments and stages. Our results demonstrated that microbial pathogens readily adhered to the Carbothane driveline materials. The initial adherence, at least for *S. aureus* and *S. epidermidis*, however, failed to convert into mature biofilms in a drip-flow biofilm reactor that mimics the driveline exit site environment. This may explain the low incidence of exit site infections associated with the Carbothane driveline recently reported by Ravichandran *et al.* (2020) [14]. A comparison using our previous data of the Pellethane driveline [10] and current results suggested an evident difference between these two drivelines in supporting mature biofilm growth. Unlike the Pellethane driveline, the Carbothane driveline

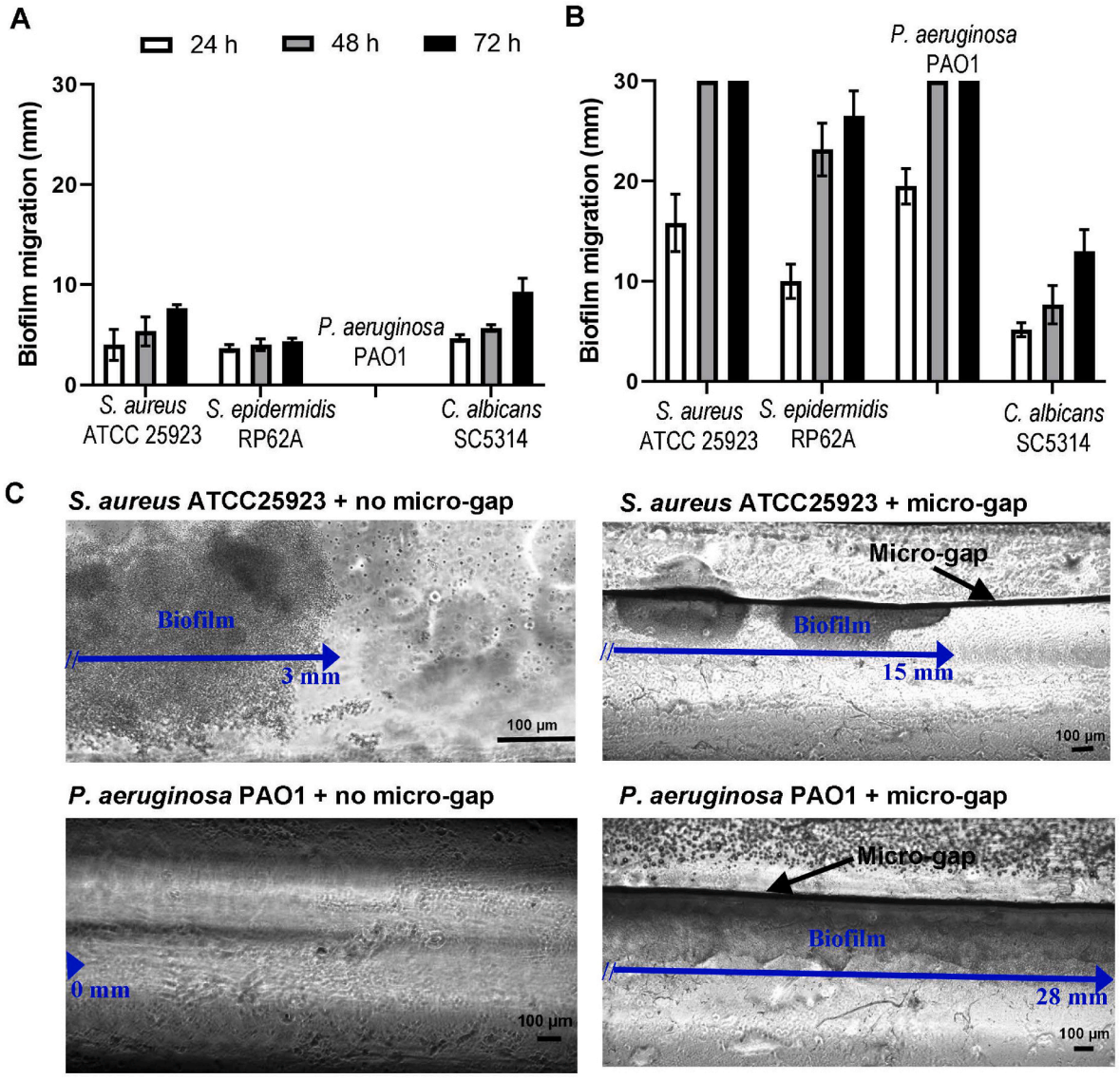

Fig. 4. Biofilm migration at the Carbothane driveline-tunnel interface. Biofilm migration of four model microorganism in tightly enclosed tunnels (A) or tunnels with micro-gaps (B) was quantitatively assessed by measuring migration distances at 24-h intervals using a wide-field microscope. (C) Overnight microscopic monitoring of biofilm migration in driveline tunnels with or without micro-gaps for *S. aureus* and *P. aeruginosa*. The presence of micro-gaps in the driveline tunnel promoted biofilm migration of both *S. aureus* and *P. aeruginosa* along the driveline surface. Blue lines with arrows indicate biofilm growths in the tunnel and the distance that biofilms migrated from the left end of the tunnel to the right side. Six biological repeats were carried out and representative images (C) were presented. (For interpretation of the references to colour in this figure legend, the reader is referred to the Web version of this article.)

Table 1
Elemental surface concentration of different Carbothane driveline components as determined by X-ray photoelectron spectroscopy.

	Atomic%	
	Smooth section (mean ± SD)	Velour (mean ± SD)
Carbon	55.3 ± 4.4	65.9 ± 0.6
Fluorine	15.8 ± 6.1	2.6 ± 1.7
Oxygen	18.3 ± 3.0	23.8 ± 1.7
Silicon	10.3 ± 1.4	7.5 ± 3.1
Nitrogen	0.3 ± 0.1	0.3 ± 0.0

*SD, Standard deviation.

smooth section, which is routinely placed at the exit site, failed to sustain the low number of pre-attached staphylococcal cells under a moderately dynamic condition.

It has been reported that the mechanical driveline features of drivelines may have impacts on the incidence of driveline infections [16,27]. There was no significant change in the outer diameter between the Pellethane driveline and the Carbothane driveline. The Carbothane driveline has a stiffness similar to what was reported for the 200 mm distal section of the silicone-based HMII driveline [16]. Size and stiffness of drivelines were thought to be linked to the risk of micro-trauma at the exit site or in the tissue tunnel; smaller diameter and/or lower stiffness of the driveline may allow better healing of driveline-related anatomic sites and promote host defenses against driveline infections [14]. Our drip-flow biofilm reactor assay however, only focused on the microorganism-device interactions and pre-excluded the influence of host-defenses on microbial biofilm formation. We thus reason the anti-biofilm performance of the Carbothane driveline found in the drip-flow biofilm reactor is only related to the surface characteristics of the biomaterial.

It should also be noted that the biological response to medical devices is determined by the entire history of its surface, including effects

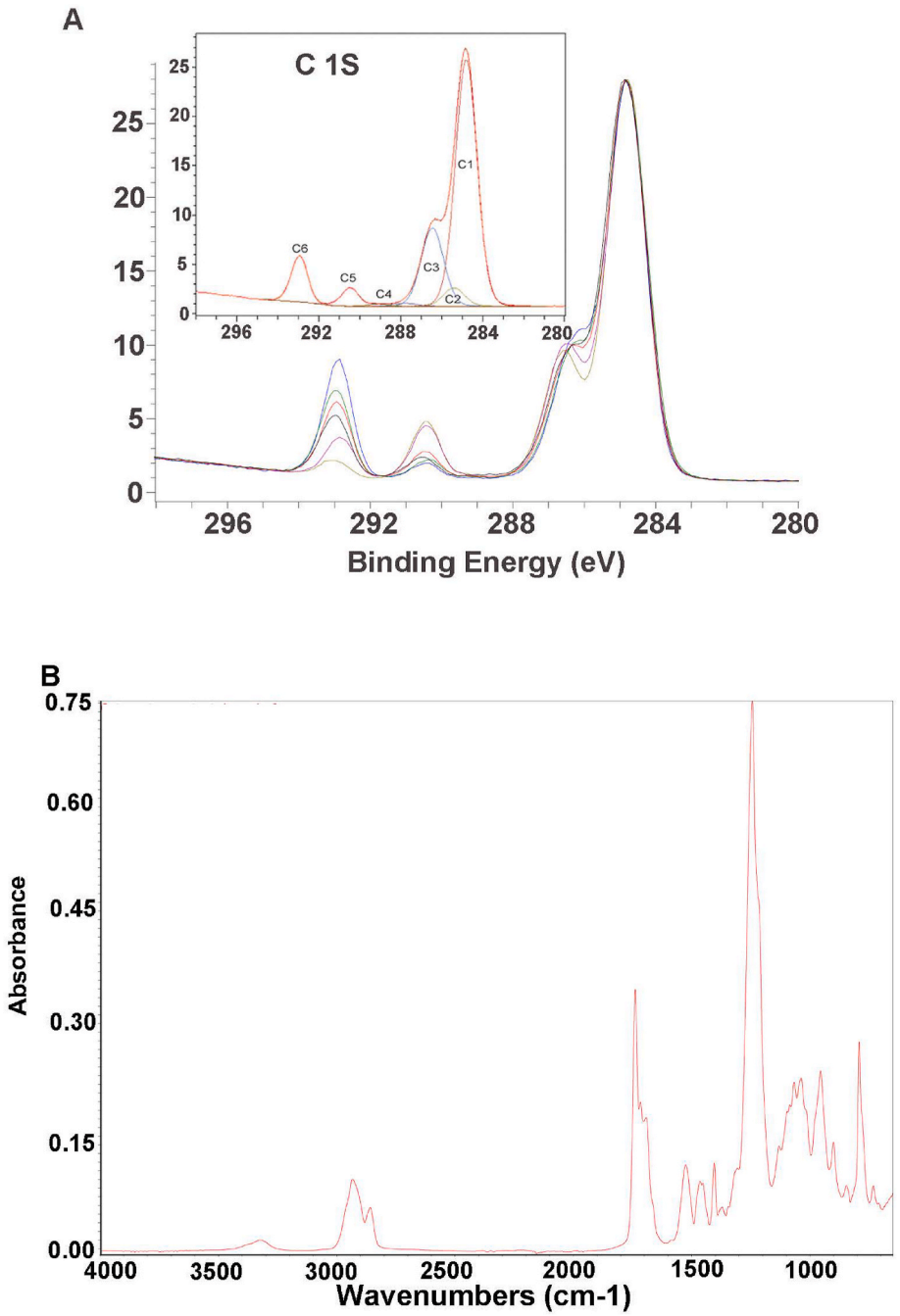

Fig. 5. High-resolution XPS spectra for the Carbonthane driveline sections**. A)** C 1s spectra of the smooth tube section, with fitted C 1s spectrum for one of the analyzed samples. B) ATR-FTIR spectra of the convex surface of the smooth section of the Carbothane driveline.

of processing steps leading to oxidation, surface contamination resulting from processing steps, sterilisation steps etc. Therefore, it should be questioned whether the high resistance of the Carbothane driveline to microbial biofilm formation is purely related to the surface chemistry of the actual Carbothane or whether it is also (or exclusively) influenced by the fluorine and/or silicon presence at the surface, as indicated by our XPS. PDMS (silicone) is a preferred biomaterial for many microorganisms to adhere and form biofilms. Its presence may compromise the anti-infective efficacy of the driveline [10]. Whether surface fluorine plays any role in the microorganism-driveline interaction needs further investigation. High hydrophobicity of both smooth and velour sections is another important surface characteristic of the Carbothane driveline that has been reported to be able to prevent microbial adherence to implanted medical devices [26].

It is a particularly interesting result that the Carbothane driveline did not support the translation of adherent staphylococcal cells to mature biofilms under a dynamic environment. Biofilm EPS is the major mediator for the formation of microcolony/macrocolony biofilms [28, 29]. Our previous work using the Pellethane HVAD driveline and other biomedical materials confirmed that the staphylococcal strains selected for this study could readily produce biofilm EPS under similar environmental conditions [10]. We thus speculated that the specific surface chemistry of the Carbothane driveline, possibly the presence of aliphatic function groups or fluorine, might have allowed single staphylococcal cells to attach but prevented anchoring of the EPS and the build-up of mature biofilms. Our CLSM study provided visual evidence to support the lower capability of the new Carbothane, relative to the Pellethane material, to allow staphylococcal biofilm EPS to attach on its surface.

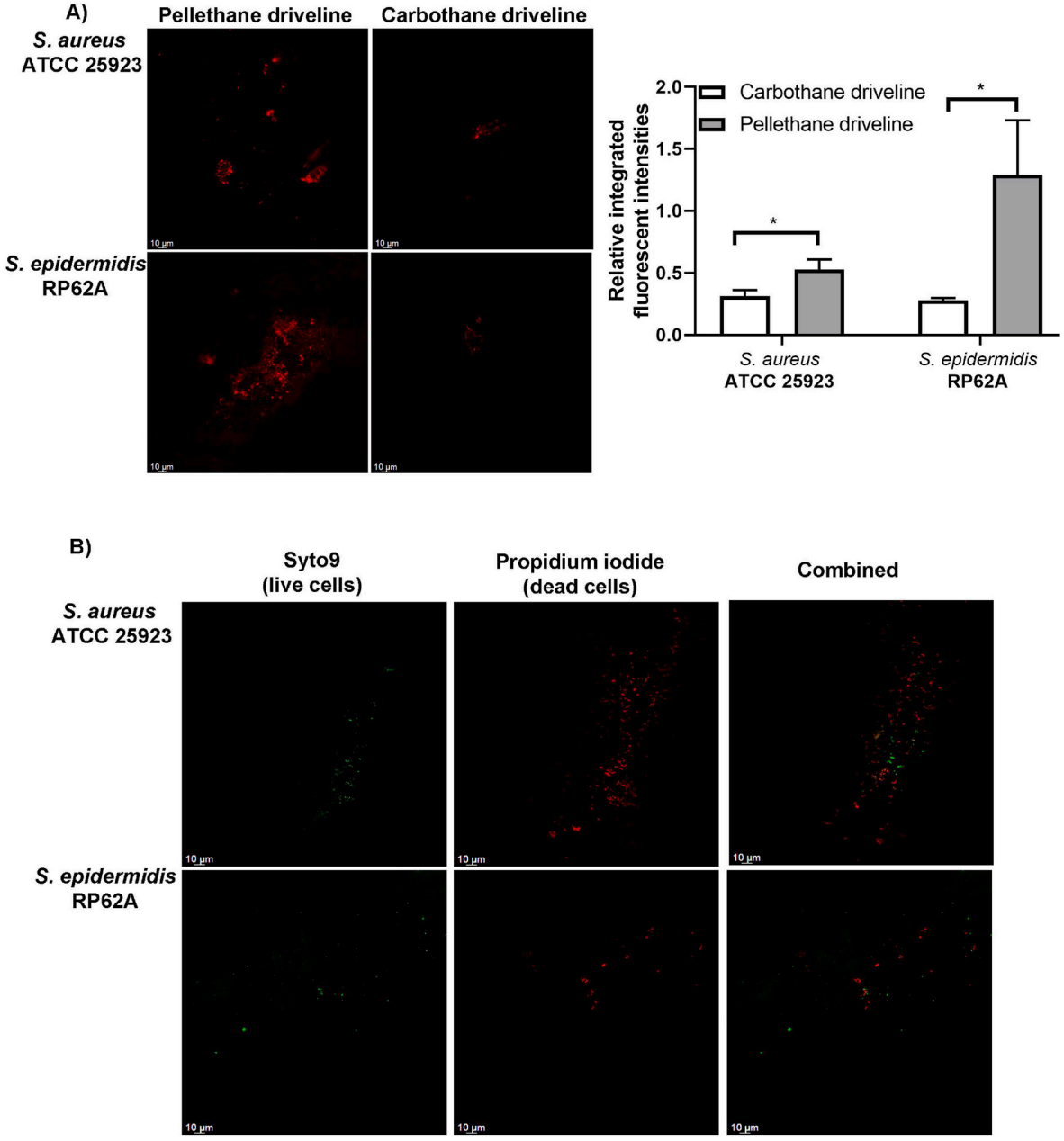

Fig. 6. A) Attachment of staphylococcal biofilm EPS to driveline smooth tubes. EPS of *S. aureus* ATCC 25923 and *S. epidermidis* RP62A biofilms was extracted, and the soluble extract was incubated with either the Carbothane driveline or the Pellethane driveline smooth tubes for 24 h, followed by wheat germ agglutinin (WGA) staining and confocal laser scanning microscopy. Relative integrated fluorescence intensity of immobilized EPS was measured by ImageJ. A significantly larger amount of EPS was found to be immobilized to the Pellethane driveline smooth section than the Carbothane driveline ($p = 0.021$ for *S. aureus*, and $p = 0.05$ for *S. epidermidis*). Experiments were carried out in five biological repeats. Error bars represent standard error of means. B) Live/dead staining of staphylococcal cells attached to Carbothane driveline smooth sections. Green signals (Syto9) represent live cells and red signals (propidium iodide) represent dead cells. Images were taken at a high magnification of 630x. (For interpretation of the references to colour in this figure legend, the reader is referred to the Web version of this article.)

The resistance of the Carbothane driveline to biofilm EPS deposition may result in reduced biofilm formation and less biofilm-related infections at the driveline exit site. In addition, partial bacterial killing upon contact with the surface was observed for the Carbothane driveline smooth section. This contact killing is possibly due to the presence of fluorine in the surface of the Carbothane material [30] but future work is required to systemically study the interaction between Carbothane driveline materials, staphylococci, and different biofilm EPS in a quantitative manner.

Despite the anti-EPS-anchoring and antibacterial properties of the Carbothane material, the presence of a driveline tunnel was able to promote staphylococcal biofilm formation on the Carbothane driveline surface. Biofilm formation of *Staphylococcus* spp. within the driveline tunnel was supported by the presence of an interstitial space between the driveline and the tissue tunnel that might trap the produced EPS in a confined space, as well as micro-gaps in the velour. Beside microbial early adherence and biofilm formation, biofilm migration in the tissue tunnel is another concern as it is clinically associated with disease severity [7]. Limited biofilm migration at the driveline-tunnel interface was noticed when the tunnel was tightly sealed (this study and [10]). We have previously revealed the presence of micro-gaps at the driveline-tunnel interface in patients with a VAD and speculated that these micro-gaps facilitated biofilm migration in the driveline tunnel to deeper tissues [7]. Findings from this *in vitro* study validated our

speculation of the role of micro-gaps in the spread of infections.

In conclusion, we experimentally studied the anti-infective performance of the Carbothane driveline and analyzed multiple physicochemical features that might adversely affect microbial adherence and biofilm formation. Although Medtronic has withdrawn the HVAD system from the market, the strategy of using Carbothane as an anti-infective biomaterial may be transferred to many other medical devices, such as central venous catheters, ECMO cannulae, and peritoneal dialysis catheters to combat problematic biofilm-related infections. However, in each case it is essential to pay close attention to the chemistry at the outermost device surface, as the entire processing history of a device, including contaminants will contribute to the biological response.

Sources of funding

This work was financially supported by a Medtronic External Research Program to YQ, DM, AP and HT.

CRediT authorship contribution statement

Yue Qu: Conceptualization, Funding acquisition, Writing – original draft, Experimentation, Methodology, Validation, Writing – review & editing. **David McGiffin:** Conceptualization, Funding acquisition, Writing – review & editing. **Lina Duque Sanchez:** Experimentation, Methodology, Validation, Writing – review & editing. **Thomas Gengenbach:** Experimentation, Methodology, Validation, Writing – review & editing. **Chris Easton:** Experimentation, Methodology, Validation, Writing – review & editing. **Helmut Thissen:** Funding acquisition, Writing – review & editing. **Anton Y. Peleg:** Conceptualization, Funding acquisition, Writing – review & editing.

Declaration of competing interest

Dr. Yue Qu, Prof. David McGiffin, Dr. Helmut Thissen, and Prof. Anton Peleg received a Medtronic External Research Program that financially supported this study. Medtronic played no direct role in the design of the study, interpretation of the results, and writing-up the manuscript. Prof. David McGiffin is a proctor for Abbott-implantation of HeartMate III ventricular assist device.

Data availability

Data will be made available on request.

Acknowledgements

The authors thank Medtronic for funding support and Monash Micro Imaging and Monash Ramaciotti Cryo EM Facility for the assistance with microscopy.

Appendix A. Supplementary data

Supplementary data to this article can be found online at https://doi.org/10.1016/j.bioflm.2023.100124.

References

[1] Schramm R, et al. Current perspectives on mechanical circulatory support. Eur J Cardio Thorac Surg 2019;55(Suppl 1):i31–7.
[2] Patel CB, Cowger JA, Zuckermann A. A contemporary review of mechanical circulatory support. J Heart Lung Transplant 2014;33(7):667–74.
[3] Qu Y, Peleg AY, McGiffin D. Ventricular assist device-specific infections. J Clin Med 2021;10(3).
[4] Leuck AM. Left ventricular assist device driveline infections: recent advances and future goals. J Thorac Dis 2015;7(12):2151–7.
[5] Pereda D, Conte JV. Left ventricular assist device driveline infections. Cardiol Clin 2011;29(4):515–27.
[6] Qu Y, et al. Percutaneous and transcutaneous connections. In: Gregory SD, Stevens MC, Fraser JF, editors. Mechanical circulatory and respiratory support. Academic Press; 2018. p. 659–89.
[7] Qu Y, et al. Characterization of infected, explanted ventricular assist device drivelines: the role of biofilms and microgaps in the driveline tunnel. J Heart Lung Transplant; 2020.
[8] Toba FA, et al. Role of biofilm in Staphylococcus aureus and Staphylococcus epidermidis ventricular assist device driveline infections. J Thorac Cardiovasc Surg 2011;141(5):1259–64.
[9] Pinninti M, Thohan V, Sulemanjee NZ. Driveline insulation as a conduit for left ventricular assist device pocket infection. J Thorac Cardiovasc Surg 2014;148(1):e135–6.
[10] Qu Y, et al. Biofilm formation and migration on ventricular assist device drivelines. J Thorac Cardiovasc Surg 2020;159(2):491–502.
[11] Trachtenberg BH, et al. A review of infections in patients with left ventricular assist devices: prevention, diagnosis and management. Methodist Debakey Cardiovasc J 2015;11(1):28–32.
[12] Bomholt T, et al. Driveline infections in patients supported with a HeartMate II: incidence, aetiology and outcome. Scand Cardiovasc J 2011;45(5):273–8.
[13] MedTronic, *HVAD system Carbothane driveline brochure*. 2020.
[14] Ravichandran AK, et al. An analysis of driveline infections with left ventricular assist devices utilizing carbothane versus pellethane driveline sheaths. J Heart Lung Transplant 2021;40(4):S434–5.
[15] Goeres DM, et al. A method for growing a biofilm under low shear at the air-liquid interface using the drip flow biofilm reactor. Nat Protoc 2009;4(5):783–8.
[16] Imamura T, et al. Correlation between driveline features and driveline infection in left ventricular assist device selection. J Artif Organs 2017;20(1):34–41.
[17] Qu Y, et al. Searching for new strategies against polymicrobial biofilm infections: guanylated polymethacrylates kill mixed fungal/bacterial biofilms. J Antimicrob Chemother 2016;71(2):413–21.
[18] Taff HT, et al. A Candida biofilm-induced pathway for matrix glucan delivery: implications for drug resistance. PLoS Pathog 2012;8(8):e1002848.
[19] Qu Y, et al. Densely adherent growth mode, rather than extracellular polymer substance matrix build-up ability, contributes to high resistance of Staphylococcus epidermidis biofilms to antibiotics. J Antimicrob Chemother 2010;65(7):1405–11.
[20] CLSI, *Clinical and Laboratory Standards Institute*. Performance standards for antimicrobial susceptibility testing. Twenty-eight Informational Supplement M100; 2018.
[21] Qu Y, et al. Hyperosmotic infusion and oxidized surfaces are essential for Biofilm Formation of Staphylococcus capitis from the neonatal intensive care unit. Front Microbiol 2020;11:920.
[22] Hook AL, et al. Combinatorial discovery of polymers resistant to bacterial attachment. Nat Biotechnol 2012;30(9):868–75.
[23] Beamson G, Briggs D. High resolution XPS of organic polymers the scienta ESCA300 database. Chichester: Wiley; 1992.
[24] Dandeniyage LS, et al. In vitro oxidative stability of high strength siloxane poly (urethane-urea) elastomers based on linked-macrodiol. J Biomed Mater Res B Appl Biomater 2019;107(8):2557–65.
[25] Rogulska M. Polycarbonate-based thermoplastic polyurethane elastomers modified by DMPA. Polym Bull 2019;76(9):4719–33.
[26] Hook AL, et al. Combinatorial discovery of polymers resistant to bacterial attachment. Nat Biotechnol 2012;30(9):868–75.
[27] Kranzl M, et al. Driveline features as risk factor for infection in left ventricular assist devices: meta-analysis and experimental tests. Front Cardiovasc Med 2021;8:784208.
[28] Fluckiger U, et al. Biofilm formation, icaADBC transcription, and polysaccharide intercellular adhesin synthesis by staphylococci in a device-related infection model. Infect Immun 2005;73(3):1811–9.
[29] O'Gara JP. Ica and beyond: biofilm mechanisms and regulation in Staphylococcus epidermidis and Staphylococcus aureus. FEMS Microbiol Lett 2007;270(2):179–88.
[30] Chen M, et al. Improvement in antibacterial properties and cytocompatibility of titanium by fluorine and oxygen dual plasma-based surface modification. Appl Surf Sci 2019;463:261–74.